

Spin-wave calculations for magnetic stacks with interface Dzyaloshinskii-Moriya interaction

Hedi Bouloussa, Yves Roussigné, Mohamed Belmeugeni, Andrey Stashkevich, and Salim Mourad Chérif*
Laboratoire des Sciences des Procédés et des Matériaux, CNRS-UPR 3407, Université Paris 13, Villetaneuse 93430, France

Jiawei Yu and Hyunsoo Yang

Department of Electrical and Computer Engineering, National University of Singapore 117576, Singapore



(Received 20 March 2018; revised manuscript received 12 July 2018; published 31 July 2018)

We present a complete calculation of spin waves in magnetic stacks, including the interfacial Dzyaloshinskii-Moriya interaction (iDMI) as a boundary condition, and discuss the influence of interlayer coupling and magnetic anisotropy on the spin-wave nonreciprocity. We show that the usual simple approach relating the iDMI strength to the slope of the spin-wave nonreciprocity versus the spin-wave number, in the case of a thin ferromagnetic film in contact with a heavy metal exhibiting a strong-orbit coupling, is not valid in many more complex structures. In the case of stacks made of identical magnetic layers, an analytical method allowed us to check that the effect of iDMI on the entire structure is captured by including the total thickness of the ferromagnetic layers. The experimental data obtained for some systems by means of Brillouin light scattering are analyzed through the presented models.

DOI: [10.1103/PhysRevB.98.024428](https://doi.org/10.1103/PhysRevB.98.024428)

I. INTRODUCTION

For several decades it was universally accepted that the conventional isotropic exchange interaction directly linking adjacent magnetic atoms and described by the Heisenberg's model proposed in the late 1920s is only responsible for the ferromagnetic ordering including such spectacular manifestations as the domain structure. However, in the late 1950s this fundamental item had to be reconsidered and it was shown that in low-symmetry systems lacking the inversion symmetry this description is incomplete and an antisymmetric term has to be added, as predicted by Dzyaloshinskii from purely symmetric grounds [1]. Contrary to the Heisenberg term imposing the parallel spin arrangement, this additional contribution accounts for the antisymmetric exchange interaction that favors noncollinear orientation of neighboring spins. Theory has so far proposed several mechanisms of the anisotropic exchange mechanism generally referred to as the Dzyaloshinskii-Moriya interaction (DMI). While Moriya [2] has suggested that in low-symmetry dielectrics it can be seen as the combined effect of the spin-orbit interaction (SOI) and conventional exchange, a different mechanism was put forward by Fert and Levy [3] to explain a peculiar magnetic behavior of spin glasses with nonmagnetic (NM) heavy-metal impurities. The experimentally observed enhancement of the anisotropy field was proposed to arise from an additional term in the Ruderman-Kittel-Kasuya-Yosida (RKKY) interaction of the Dzyaloshinskii-Moriya type, due to spin-orbit scattering of the conduction electrons by the nonmagnetic impurities. Importantly, both proposed mechanisms rely on the SOI. In this respect, a bilayer composed of a heavy metal (HM) and ferromagnetic metal (FM) seems to be exceptionally promising. In this structure the high SOI efficiency is ensured

by the presence of a heavy metal while an interface provides the required symmetry reduction, as suggested by Fert [4]. As a result, the DMI is localized in the close vicinity of the HM/FM interface and thus is referred to as interface DMI (iDMI).

iDMI is widely studied nowadays because it generates particular magnetization configurations like chiral walls or skyrmions that could be used for information storage [5–9]. It has been shown recently that skyrmions can be stabilized and manipulated at room temperature in magnetic multilayers by tailoring the magnetic interactions governing their properties [10–16]. In particular, it was revealed that the Néel-type domain-wall chirality imposed by iDMI is instrumental in high-speed manipulating of magnetization with spin-torque currents in ultrathin FM films, that are at the heart of the present applications in spintronics. Thus, in systems with iDMI, large magnetic domain-wall velocities have been observed, both in current-driven experiments as well as in field-driven ones [9,17–21].

Further iDMI related improvement of performance of spintronic devices can be achieved in HM/FM/HM trilayers taking advantage of potential addition of contributions from two interfaces [11,22,23]. However, the iDMI symmetry is such that this is only possible if intrinsic iDMIs at these interfaces have opposite signs. At the same time, despite a considerable number of studies [9,24–28], the relationship between iDMI (strength and sign) and the interface structure remains not yet fully understood to the point that theoretical predictions [29] are sometimes in contradiction with experimental results both in sign and intensity of iDMI coupling.

Multilayer stacks with an *ad hoc* number of layers and *ad hoc* combination of physical properties of individual constitutive layers will allow for optimizing the multilayer's performance for a specific application though various intralayer and interlayer magnetic interactions, not necessarily of the exchange type. Thus the use of two separated FM “substacks,” each of them comprised of two

*cherif@univ-paris13.fr

different ferromagnets (FM = Ni/Co/Ni) in a Pt(5 nm)/FM/Au(*d*)/FM/Pt(5 nm) multilayer stack [15] gives more freedom to tune the stray fields through long-range dipolar interactions. Finally, the RKKY-type interlayer exchange coupling between two FM layers, with its sign and intensity tunable through the thickness of a conducting metal spacer, is another cornerstone of modern spintronics whose functional possibilities should not be overlooked.

The purpose of this paper is to explore, mainly theoretically, the major features in the dynamic behavior of magnetization in multilayer stacks taking in account the full set of interactions. They include both short-range exchange related magnetic coupling, namely the conventional bulk intralayer isotropic exchange, iDMI localized at FM/HM interfaces, and RKKY interlayer interaction coupling neighboring FM films, as well as long-range interactions of dipolar nature. Theoretical component of the research will focus on low-amplitude dynamics of the studied systems, in other words on dipole-exchange spin waves that reflect major features of system's dynamic behavior in general. Experimentally, we rely on Brillouin light scattering (BLS) spectroscopy, a powerful and reliable instrument of characterization in spintronics whose high effectiveness, demonstrated in experimental papers by Grünberg [30–33] of RKKY-related artificial antiferromagnets, and confirmed in numerous publications that followed.

Recently this technique has proven to be very efficient for measuring the strength of iDMI and its sign. In fact, the iDMI constant is directly proportional to the frequency difference observed for two spin waves propagating in opposite directions, perpendicularly to the static magnetization [34–38], namely the Stokes $f(-k)$ and anti-Stokes $f(k)$ frequencies. This feature is reproduced in spin-wave behavior in thin ferromagnetic films (FM) in contact with a single heavy metal (HM) layer possessing a strong spin-orbit coupling. But, how does iDMI modify the spin-wave frequency for more complex magnetic multilayer stacks? The aim of this study is to evaluate this influence for these structures that are expected to be important for developing future ultrahigh density storage and logic devices.

The model we used for deriving spin-wave dispersion relations in magnetic layers is close to the one presented in Ref. [39] based on a continuum-type magnetostatic theory including both dipolar and exchange contributions and fully taking into account magnetic surface and interface anisotropies as well as interlayer exchange coupling. The difference consists in imposing additional iDMI related boundary conditions on circular components of the dynamic magnetization as proposed in Ref. [40], where it was shown that iDMI leads to additional pinning at the interface and that the iDMI-based pinning scales as the spin-wave number.

iDMI is an interfacial effect. Thus, the introduction of this term in the Landau-Lifshitz (LL) equation results from an approximation obtained by averaging the LL equation over the thickness. Including iDMI directly in the LL equation is not always possible. For example, the averaging cannot provide the Stokes/anti-Stokes frequency difference due to different usual pinning conditions (related to surface anisotropy) on the two sides of a film. Consequently, a full calculation (without averaging) is necessary to accurately evaluate the

Stokes/anti-Stokes frequency difference in presence of iDMI and different pinning conditions. In fact in most of nonsymmetrical structures, a full numerical calculation is mandatory. Our model is discussed within the framework of various stacks ranging from the simple FM/HM interface to more complex multilayer structures. Moreover we checked, thanks to an analytical calculation, that for a stack made of identical layers the effect of the iDMI on the entire structure is captured by including the total thickness of the ferromagnetic layers. The dipolar coupling to be derived in this approach is evaluated using the method proposed in [40] and based on magnetostatic Green's functions. Some experimental results obtained by BLS technique are then analyzed by means of the proposed models.

II. MODEL

A. Spin-wave equation inside a ferromagnetic layer

We consider a uniformly magnetized medium in the z direction that lies along the external magnetic field and assume a uniaxial anisotropy along the y axis perpendicular to the magnetic medium. The Landau-Lifshitz equation of motion yields [39]

$$i\frac{\omega}{\gamma}m_x = Hm_y - \frac{2K}{M}m_y - M\frac{\partial\phi}{\partial y} - \frac{2A}{M}\Delta m_y, \quad (1)$$

$$i\frac{\omega}{\gamma}m_y = -Hm_x + M\frac{\partial\phi}{\partial x} + \frac{2A}{M}\Delta m_y, \quad (2)$$

where m_x, m_y are the oscillatory components of the magnetization, ϕ is the potential associated to the demagnetizing field (also introduced in Ref. [41]), ω is the angular frequency, γ is the gyromagnetic factor, A is the exchange constant, H is the external field, M is the static magnetization, and K is the anisotropy constant. The symbol Δ is used for the Laplacian ∇^2 .

According to Eqs. (1) and (2), the oscillatory components of the magnetization obey the relations

$$\begin{aligned} & \left[\left(H - \frac{2A}{M}\Delta \right) \left(H - \frac{2A}{M}\Delta - \frac{2K}{M} \right) - \frac{\omega^2}{\gamma^2} \right] m_x \\ & = M \left[\left(H - \frac{2A}{M}\Delta - \frac{2K}{M} \right) \frac{\partial\phi}{\partial x} - i\frac{\omega}{\gamma} \frac{\partial\phi}{\partial y} \right], \end{aligned} \quad (3)$$

$$\begin{aligned} & \left[\left(H - \frac{2A}{M}\Delta \right) \left(H - \frac{2A}{M}\Delta - \frac{2K}{M} \right) - \frac{\omega^2}{\gamma^2} \right] m_y \\ & = M \left[\left(H - \frac{2A}{M}\Delta \right) \frac{\partial\phi}{\partial y} + i\frac{\omega}{\gamma} \frac{\partial\phi}{\partial x} \right]. \end{aligned} \quad (4)$$

In order to solve Eqs. (3) and (4), Camley *et al.* [42] use an auxiliary function ψ defined by the equation

$$\left[\left(H - \frac{2A}{M}\Delta \right) \left(H - \frac{2A}{M}\Delta - \frac{2K}{M} \right) - \frac{\omega^2}{\gamma^2} \right] \psi = \phi. \quad (5)$$

The auxiliary function allows for using a unique function instead of the three functions m_x, m_y , and ϕ . It enables us to formally solve the LL equation. The remaining equation is then the Maxwell equation on the dynamic magnetic field. Another method consists in solving first the Maxwell equation, i.e., deriving the dynamic demagnetizing field from the dynamic magnetization and to use it in the LL equation. This auxiliary function allows for deriving the expressions for the oscillatory

components of the magnetization as

$$m_x = M \left[\left(H - \frac{2A}{M} \Delta - \frac{2K}{M} \right) \frac{\partial \psi}{\partial x} - i \frac{\omega}{\gamma} \frac{\partial \psi}{\partial y} \right], \quad (6)$$

$$m_y = M \left[\left(H - \frac{2A}{M} \Delta \right) \frac{\partial \psi}{\partial y} + i \frac{\omega}{\gamma} \frac{\partial \psi}{\partial x} \right]. \quad (7)$$

Replacing in the Maxwell equation $\Delta \phi + 4\pi \left(\frac{\partial m_x}{\partial x} + \frac{\partial m_y}{\partial y} \right) = 0$, the oscillatory magnetization, and the potential by their expressions (5)–(7), we obtain the wave equation

$$\begin{aligned} & \left[\left(H - \frac{2A}{M} \Delta \right) \left(H - \frac{2A}{M} \Delta - \frac{2K}{M} \right) - \frac{\omega^2}{\gamma^2} \right] \Delta \psi \\ & + 4\pi M \left[\left(H - \frac{2A}{M} \Delta - \frac{2K}{M} \right) \frac{\partial^2 \psi}{\partial x^2} \right. \\ & \left. + \left(H - \frac{2A}{M} \Delta \right) \frac{\partial^2 \psi}{\partial y^2} \right] = 0. \end{aligned} \quad (8)$$

B. Spin-wave dispersion relations

1. iDMI inducing FM/HM bilayer

A propagating wave along the x direction in a magnetic film perpendicular to the y axis corresponds to a $\exp(ikx)$ dependence for the function ψ . Consequently Eq. (8) becomes a linear differential equation of rank 6 with respect to y . The general solution of this equation is a linear combination of 6 $\exp(iqy)$ where q is a root of the algebraic equation associated to the differential equation. q may be real or complex. The different $\exp(iqy)$ are necessary to fulfill the boundary conditions. Thus a wave propagating along the x direction corresponds to

$\psi = \exp(ikx) [\psi_1 \exp(iq_1 y) + \dots + \psi_6 \exp(iq_6 y)]$, where $q_1 \dots q_6$ are the roots of

$$\begin{aligned} & \left\{ \left[H + \frac{2A}{M} (k^2 + q^2) \right] \left[H + \frac{2A}{M} (k^2 + q^2) - \frac{2K}{M} \right] \right. \\ & \left. - \frac{\omega^2}{\gamma^2} \right\} (k^2 + q^2) + 4\pi M \left\{ \left[H + \frac{2A}{M} (k^2 + q^2) - \frac{2K}{M} \right] k^2 \right. \\ & \left. + \left[H + \frac{2A}{M} (k^2 + q^2) \right] q^2 \right\} = 0. \end{aligned} \quad (9)$$

Above the magnetic film, the potential reads $\phi_{\text{ext}} = \phi_1 \exp(ikx) \exp(-ky)$. Below the magnetic film, the potential reads $\phi_{\text{ext}} = \phi_2 \exp(ikx) \exp(ky)$. On each interface, the Maxwell boundary conditions yield the relations

$$\frac{\partial \phi}{\partial y} + 4\pi m_y = \frac{\partial \phi_{\text{ext}}}{\partial y}, \quad (10)$$

$$\phi = \phi_{\text{ext}}. \quad (11)$$

We assume that the upper interface is characterized by pinning via conventional out-of-plane surface anisotropy while the lower interface is submitted to both iDMI and out-of-plane surface anisotropy. On the upper interface, the Rado-Weertman boundary conditions read [39]

$$\frac{2A}{M} \frac{\partial m_x}{\partial y} = 0, \quad (12)$$

$$\frac{2A}{M} \frac{\partial m_y}{\partial y} - \frac{2K_{s,\text{up}}}{M} m_y = 0, \quad (13)$$

where $K_{s,\text{up}}$ is the surface anisotropy constant.

On the lower interface, the Kostylev boundary conditions read [40]

$$\frac{2A}{M} \frac{\partial m_x}{\partial y} - i \frac{2D}{M} k m_y = 0, \quad (14)$$

$$\frac{2A}{M} \frac{\partial m_y}{\partial y} + i \frac{2D}{M} k m_x + \frac{2K_{s,\text{low}}}{M} m_y = 0, \quad (15)$$

where D is the iDMI constant and $K_{s,\text{low}}$ is the surface anisotropy constant.

At variance with Kostylev, the constant D presented in relations (14) and (15) is energy per length. This constant is the product of the Kostylev iDMI constant by the atomic distance required in his presentation. In numerous publications [34,35,43], the constant D considered here is referred to as the intrinsic or surface iDMI constant.

The boundary conditions (10) and (11) on both interfaces and (12)–(15) yield a set of eight linear equations of the unknowns $\phi_1, \phi_2, \psi_1, \psi_2, \psi_3, \psi_4, \psi_5, \psi_6$. This set of equations has nontrivial solutions only if its determinant is equal to zero. This mathematical condition corresponds to an equation that describes the dispersion characteristics of spin-wave modes in the structure.

2. RKKY-coupled FM/NM/FM trilayer on top of a HM film

The presence of the FM/HM interface at the bottom of the structure is necessary to induce the required iDMI. In each ferromagnetic layer, the oscillatory magnetization and the associated potential are derived from an auxiliary function like in the case of an isolated ferromagnetic film. The considered boundary conditions on the top interface of the upper FM layer and on the bottom interface of the lower layer are the same as those for a single magnetic film.

Within the spacer, the potential reads $\phi_{\text{spa}} = \phi_3 \exp(ikx) \exp(-ky) + \phi_4 \exp(ikx) \exp(ky)$. On each interface with the spacer, the Maxwell boundary conditions yield the relations

$$\frac{\partial \phi}{\partial y} + 4\pi m_y = \frac{\partial \phi_{\text{spa}}}{\partial y}, \quad (16)$$

$$\phi = \phi_{\text{spa}}. \quad (17)$$

Moreover the Hoffmann boundary conditions on the interfaces with the spacer are [44]

$$\frac{2A_{\text{up}}}{M_{\text{up}}} \frac{\partial m_{x,\text{up}}}{\partial y} + \frac{2A_{12}}{M_{\text{low}}} m_{x,\text{low}} - \frac{2A_{12}}{M_{\text{up}}} m_{x,\text{up}} = 0, \quad (18)$$

$$\begin{aligned} & \frac{2A_{\text{up}}}{M_{\text{up}}} \frac{\partial m_{y,\text{up}}}{\partial y} + \frac{2A_{12}}{M_{\text{low}}} m_{y,\text{low}} - \frac{2A_{12}}{M_{\text{up}}} m_{y,\text{up}} \\ & + \frac{2K_{s,\text{up}}}{M_{\text{up}}} m_{y,\text{up}} = 0, \end{aligned} \quad (19)$$

$$\frac{2A_{\text{low}}}{M_{\text{low}}} \frac{\partial m_{x,\text{low}}}{\partial y} - \frac{2A_{12}}{M_{\text{up}}} m_{x,\text{up}} + \frac{2A_{12}}{M_{\text{low}}} m_{x,\text{low}} = 0, \quad (20)$$

$$\begin{aligned} & \frac{2A_{\text{low}}}{M_{\text{low}}} \frac{\partial m_{y,\text{low}}}{\partial y} - \frac{2A_{12}}{M_{\text{up}}} m_{y,\text{up}} + \frac{2A_{12}}{M_{\text{low}}} m_{y,\text{low}} \\ & - \frac{2K_{s,\text{low}}}{M_{\text{low}}} m_{y,\text{low}} = 0, \end{aligned} \quad (21)$$

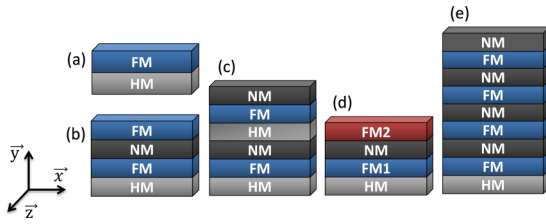


FIG. 1. A schematic of the numerically studied structures.

where *low* and *up* refer to the lower and upper films and A_{12} is the RKKY exchange constant.

The boundary conditions (10) and (11) on both outer interfaces, (12)–(15), (16) and (17) on both inner interfaces, and (18)–(21) yield a set of 16 linear equations on the unknowns $\phi_1, \dots, \phi_4, \psi_{1,low}, \dots, \psi_{6,low}, \psi_{1,up}, \dots, \psi_{6,up}$. The eigenfrequencies correspond to the vanishing of the determinant of the set of equations.

3. Multiple (NM/FM) stack on top of a HM film

In each ferromagnetic layer, the oscillatory magnetization and the associated potential are derived from an auxiliary function like in the case of an isolated ferromagnetic film. The considered boundary conditions are the same as those for two magnetic layers coupled by RKKY interaction and the bottom FM/HM interface provides introduction of the iDMI related mechanisms.

III. NUMERICAL CALCULATION RESULTS

The numerically studied structures are sketched in Fig. 1. The first structure [Fig. 1(a)] is made of a ferromagnetic layer (FM) deposited on a heavy metal (HM). The second one [Fig. 1(b)] consists in a stack FM/NM/FM/HM where NM is a metallic spacer allowing RKKY coupling. The third stack [Fig. 1(c)] is a double (NM/FM/HM) multilayer. In the fourth stack, FM₂/NM/FM₁/HM [Fig. 1(d)], the ferromagnetic layers have different magnetic parameters. Finally a stack (NM/FM)₄/HM [Fig. 1(e)] is considered.

A. Thin ferromagnetic (FM)/heavy metal (HM)

In this case the FM layer must be thin enough to make the dispersion of the dipolar mode (also called the Damon-Eshbach mode) negligible in the range of spin-wave numbers covered in the Brillouin spectroscopy. This excludes any influence on the spin-wave propagation nonreciprocity. We have calculated the spin waves' nonreciprocity for a FM/HM structure by estimating the difference between the Stokes and anti-Stokes frequencies. The calculations were performed with the following parameters: an applied magnetic field $H = 1000$ Oe, a saturation magnetization $M = 1000$ emu/cm³, an exchange constant $A = 10^{-6}$ erg/cm, a Dzyaloshinskii-Moriya constant $D = 2 \times 10^{-7}$ erg/cm, and $\frac{\gamma}{2\pi} = 3$ GHz/kOe. All the anisotropies are null. Two FM thicknesses $t_{FM} = 1$ or 2 nm were considered in order to point out the interfacial character of the Dzyaloshinskii-Moriya Interaction (iDMI) in ultrathin films. The frequency difference $f(-k) - f(k)$ for a wave number $|k|$ varying from 4 to 18 μm^{-1} is calculated (Fig. 2). As expected [34–38], the iDMI is completely responsible for

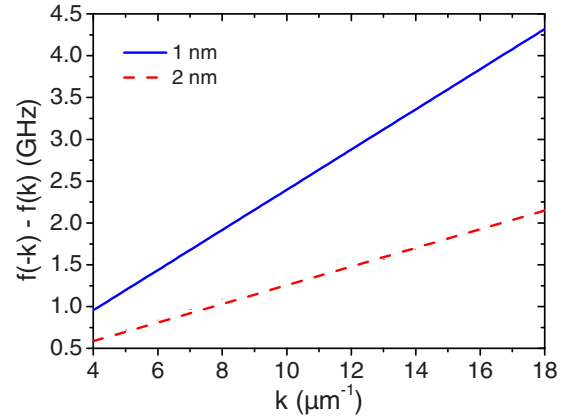


FIG. 2. Stokes/anti-Stokes frequency difference for thin FM/HM vs the in-plane wave number with $t_{FM} = 1$ nm (continuous line), $t_{FM} = 2$ nm (dashed line).

the frequency difference $f(-k) - f(k) = \frac{2\gamma}{\pi M} \frac{D}{t_{FM}} k$. The case of the single FM/HM structure is considered as a reference configuration facilitating analysis of the results concerning more complex stacks.

B. Thick ferromagnetic (FM)/heavy metal (HM)

The structures studied in the previous section were made of ultrathin films ($t_{FM} = 1$ or 2 nm) and no surface anisotropy was considered. For ultrathin films, the surface anisotropy does not yield a measurable frequency difference $f(-k) - f(k)$ [43]. Conversely if the film thickness is of a few tens of nanometers the Damon-Eshbach dispersion is no longer negligible, the distribution of the dynamic magnetization across the FM layer becomes inhomogeneous, and the surface anisotropy engenders a frequency difference commensurable with the one due to iDMI. We have performed the calculations for the thick FM/HM structure using the following parameters: $H = 1000$ Oe, $M = 1000$ emu/cm³, $A = 10^{-6}$ erg/cm, $\frac{\gamma}{2\pi} = 3$ GHz/kOe, $D = 2 \times 10^{-7}$ erg/cm, $t_{FM} = 20$ nm, and $K = 0$. Two surface anisotropies were considered: $K_{s,low} = 0$ and 0.4 erg/cm². For a thicknesses as large as 20 nm, several modes are observable by the BLS technique. The lowest mode is the dipolar mode and the other modes are the standing modes across the thickness [39]. The eigenfrequency differences for a wave number $|k|$ varying from 4 to 18 μm^{-1} were calculated. Figure 3(a) shows the results obtained for $K_{s,low} = 0$. In this case, the Damon Eshbach frequency difference $f_{DE}(-k) - f_{DE}(k)$ is given by the usual expression $\frac{2\gamma}{\pi M} \frac{D}{t_{FM}} k$ (circles) while the first standing mode frequency difference $f_{st,1}(-k) - f_{st,1}(k)$ is greater than $\frac{2\gamma}{\pi M} \frac{D}{t_{FM}} k$. For $K_{s,low} = 0.4$ erg/cm², the Damon Eshbach frequency difference is largely increased while the first standing mode frequency difference is slightly decreased, as illustrated in Fig. 3(b). It appears from the above results that the evaluation of the iDMI constant is more complex for a thick ferromagnet on a heavy metal. It requires the determination of the surface anisotropy. The Damon-Eshbach frequencies and the first standing mode frequencies allow for deriving the iDMI constant in these structures. Nevertheless the iDMI constant should be easier to evaluate from the first standing

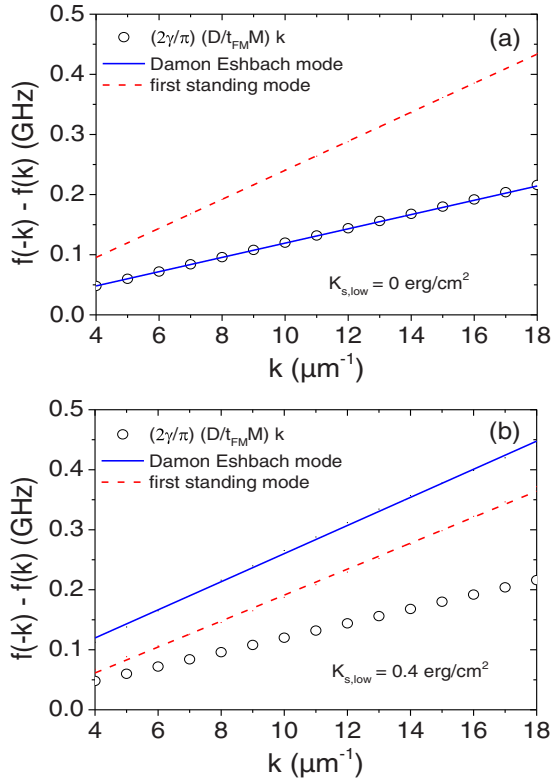


FIG. 3. Stokes/anti-Stokes frequency differences for thick FM/HM vs the in-plane wave number for two different surface anisotropies, (a) $K_{s,low} = 0 \text{ erg/cm}^2$, (b) $K_{s,low} = 0.4 \text{ erg/cm}^2$; circles indicate the frequency difference obtained with the usual expression $\frac{2\gamma}{\pi} \frac{D}{M_{FM}} k$.

mode frequency difference because this frequency difference is less sensitive to the usual surface anisotropy.

In fact, as we do not have an explicit formula for the frequency difference when different usual pinning conditions (related to surface anisotropy) are involved on the two sides of a film, a numerical calculation had been performed. The parameters used in this calculation can be modified in order to fit experimental data. Consequently both Damon-Eshbach and standing modes frequency differences allow for estimating iDMI. Nevertheless, as the Damon-Eshbach mode frequency difference is more sensitive to the difference of pinning conditions, it is easier to estimate iDMI from the standing modes frequency difference.

C. Ferromagnetic (FM)/normal metal (NM)/ferromagnetic (FM)/heavy metal (HM)

In analogy with coupled harmonic oscillators, the magnon modes in two ferromagnetic films coupled via a nonmagnetic interlayer can be classified into acoustic (dipolar) and optic (exchange) modes depending on whether the two film magnetizations precess in phase or out of phase, respectively. The interlayer exchange A_{12} depends upon the interlayer spacer in a nontrivial way: in many cases an oscillatory variation has been reported [45,46]. It is often interpreted in terms of a Ruderman-Kittel-Kasuya-Yosida (RKKY) mechanism [47]. In the following, we consider two identical FM layers separated

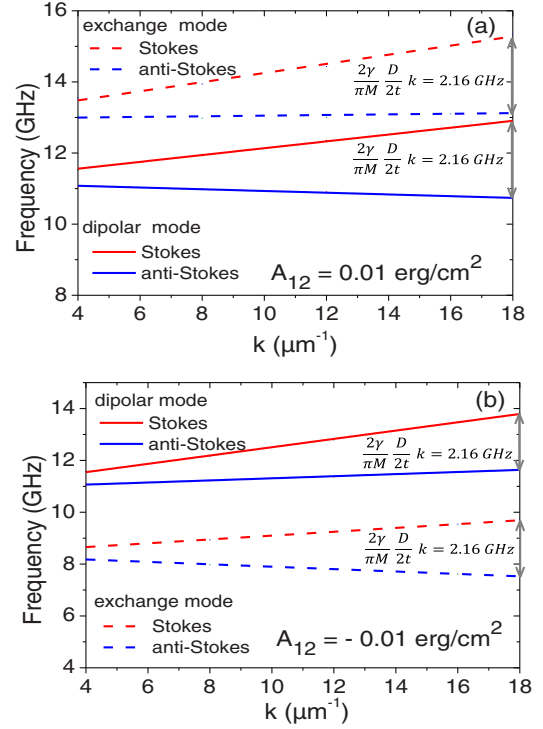


FIG. 4. Stokes and anti-Stokes frequencies for FM/NM/FM/HM vs the in-plane wave number for (a) positive interlayer exchange $A_{12} = 0.01 \text{ erg/cm}^2$, (b) negative interlayer exchange $A_{12} = -0.01 \text{ erg/cm}^2$; arrows indicate the value of the frequency difference deduced from the intuitive expression for FM/NM/FM/HM $\frac{2\gamma}{\pi} \frac{D}{2t} k$.

by a nonmagnetic metal (NM) and where the bottom FM layer is in contact with a heavy metal (HM).

The eigenfrequencies of the coupled modes in this FM/NM/FM/HM stack were calculated for $H = 1000 \text{ Oe}$, $M = 1000 \text{ emu/cm}^3$, $A = 10^{-6} \text{ erg/cm}$, $K = 0 \text{ erg/cm}^3$, all $K_s = 0 \text{ erg/cm}^2$, $t_{\text{top}} = t_{\text{bottom}} = t = 1 \text{ nm}$, $D = 2 \times 10^{-7} \text{ erg/cm}$, $\frac{\gamma}{2\pi} = 3 \text{ GHz/kOe}$. The frequency variations with the wave number for a positive exchange coupling $A_{12} = 0.01 \text{ erg/cm}^2$ and for a negative exchange coupling $A_{12} = -0.01 \text{ erg/cm}^2$ are displayed in Figs. 4(a) and 4(b), respectively. It should be noticed that for $A_{12} = 0.01 \text{ erg/cm}^2$ and $A_{12} = -0.01 \text{ erg/cm}^2$, the so-called dipolar mode (insensitive to A_{12}) shows a large difference $f(-k) - f(k)$ as well as the so-called exchange mode (A_{12} dependent) [39]. These differences coincide with $\frac{2\gamma}{\pi M} \frac{D}{2t} k$ which corresponds to the half difference for a single film of thickness t . Finally the iDMI effect should be easy to quantify for a FM/NM/FM/HM structure like in the case of FM/HM bilayer.

D. Double [normal metal (NM)/ferromagnetic (FM)/heavy metal (HM)]

We assume that all the FM layers have the same magnetic and geometric parameters. As previously discussed in Sec. III C, the stack FM/NM/FM/HM presents a Stokes/anti-Stokes frequency difference equal to the half expected difference for one FM layer on HM layer, $\delta F_{FM/NM/FM/HM} = \frac{1}{2} \delta F_{FM/HM}$. This frequency difference is mode independent (i.e., the same for the dipolar and exchange modes) and is

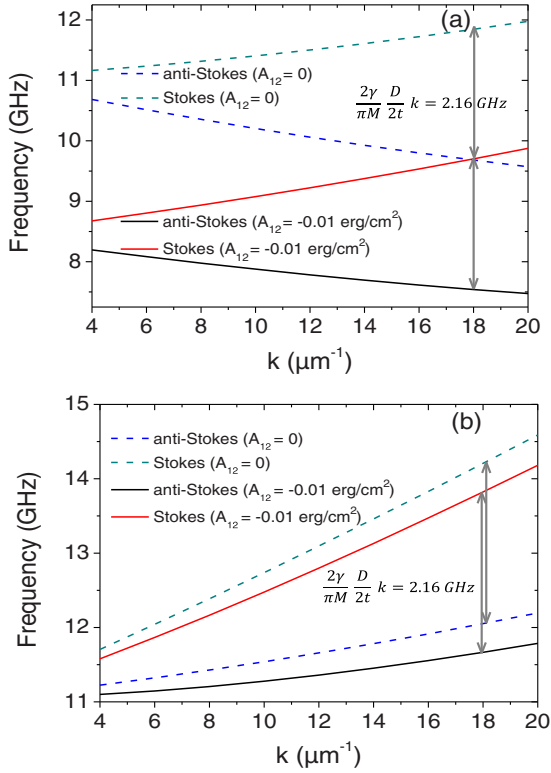


FIG. 5. Frequency vs wave number, (a) exchange mode of FM/NM/FM/HM for $A_{12} = 0$ or -0.01 erg/cm², (b) dipolar mode of FM/NM/FM/HM for $A_{12} = 0$ or -0.01 erg/cm²; arrows indicate the value of the frequency difference deduced from the intuitive expression for FM/NM/FM/HM $\frac{2\gamma}{\pi} \frac{D}{2tM} k$.

RKKY independent for identical FM layers. The numerical calculations for (NM/FM/HM)₂ show that the frequency difference has the same value as that for a single FM layer on a HM layer, $\delta F_{(NM/FM/HM)_2} = \delta F_{FM/HM}$, whatever the value of the RKKY exchange. This result is expected since in the case of a (NM/FM/HM)₂, the total magnetic thickness is the double of that for (NM/FM/HM) as well as the iDMI coupling, thus yielding the same D/t ratio in both cases. The Stokes and anti-Stokes frequencies variation with respect to the wave number are displayed in Figs. 5 and 6. The calculations are performed using the following parameters: $M = 1000$ emu/cm³, $K = 0$ erg/cm³, all $K_s = 0$ erg/cm², $A = 10^{-6}$ erg/cm, $\gamma/2\pi = 3$ GHz/kOe, $t = 1$ nm, $H = 1000$ Oe, $A_{12} = 0$ or -0.01 erg/cm², $D = 2 \times 10^{-7}$ erg/cm. As discussed above, $\delta F_{(NM/FM/HM)_2} = \delta F_{FM/HM} = 2\delta F_{FM/NM/FM/HM}$ for both modes and for any value of A_{12} . It is interesting to notice that the asymmetry of the stack FM/NM/FM/HM is revealed through the little influence of A_{12} on the dipolar frequency. In the case of the stack (NM/FM/HM)₂, the dipolar frequency keeps the same value whatever the value of A_{12} .

E. Ferromagnetic (FM₂)/normal metal (NM)/ferromagnetic (FM₁)/heavy metal (HM)

In this section, we consider two different ferromagnetic layers FM₁ and FM₂ with the bottom FM₁ magnetic layer in contact with the heavy metal. The eigenfrequencies of the coupled modes in the FM₂/NM/FM₁/HM stack were cal-

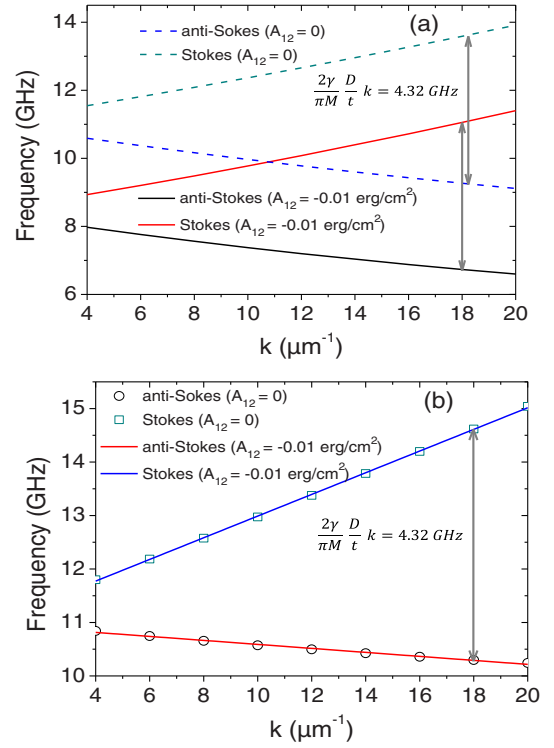


FIG. 6. Frequency vs wave number, (a) exchange mode of (NM/FM/HM)₂ for $A_{12} = 0$ or -0.01 erg/cm², (b) dipolar mode of (NM/FM/HM)₂ for $A_{12} = 0$ or -0.01 erg/cm², arrows indicate the value of the frequency difference deduced from the intuitive expression for FM/NM/FM/HM $\frac{2\gamma}{\pi} \frac{D}{tM} k$.

culated for $H = 1000$ Oe, $M_1 = 1000$ emu/cm³, $M_2 = 500$ emu/cm³, $A = 10^{-6}$ erg/cm, $t_{FM_1} = t_{FM_2} = 1$ nm, $D = 2 \times 10^{-7}$ erg/cm, and $\frac{\gamma}{2\pi} = 3$ GHz/kOe. All the anisotropies are null. The frequency difference variations with the wave number for an exchange coupling $A_{12} = 0.01$ erg/cm² are displayed in Fig. 7(a). Circles indicate the frequency difference corresponding to the mean properties $\delta f_{\text{mean}} = \frac{2\gamma}{\pi} \frac{D}{t_{FM_1} M_1 + t_{FM_2} M_2} k$. For the considered parameters, neither dipolar nor exchange frequency difference are close to δf_{mean} . The lowest (highest) frequency mode is the dipolar (exchange) mode. One can observe that the highest frequency related to the exchange mode shows a large difference frequency $f(-k) - f(k)$ while the lowest frequency difference associated to the dipolar mode is much lower. It is to be noticed that the profile of the dipolar mode is nearly uniform while the dynamic magnetization for the exchange mode has different signs in the two layers. Consequently the signal intensity of the BLS line associated to the dipolar mode is much higher than the one corresponding to the exchange mode. Consequently the iDMI effect should be evaluated from the dipolar mode frequency difference. It would have been easier to quantify it from the largest frequency difference, i.e., from the exchange mode frequency difference. Another difficulty about the iDMI evaluation for a FM₂/NM/FM₁/HM stack arises: the frequency difference also depends on the exchange coupling A_{12} . The frequency difference variations with the exchange coupling for $|k| = 18$ μm⁻¹ are displayed in Fig. 7(b). Circles indicate δf_{mean} . As A_{12} increases, the difference $f_1(-k) - f_1(k)$ for the dipolar

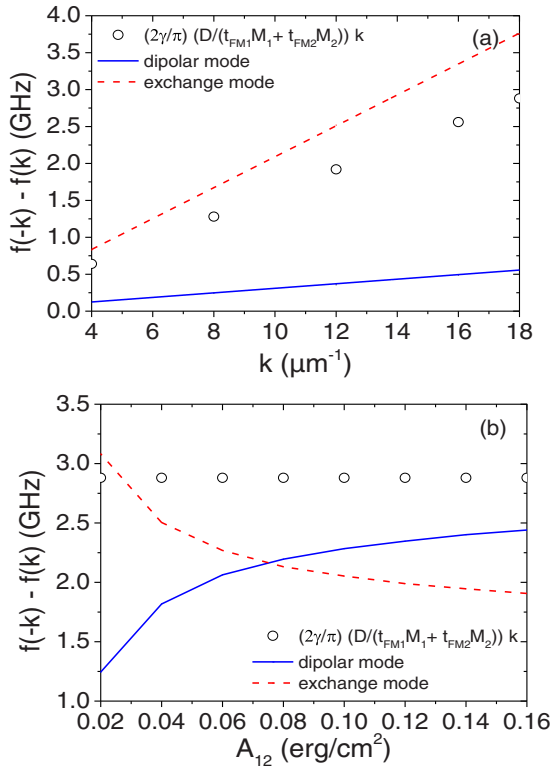


FIG. 7. Frequency difference for FM₂/NM/FM₁/HM, (a) $A_{12} = 0.01$ erg/cm², $4 \mu\text{m}^{-1} < |k| < 18 \mu\text{m}^{-1}$, (b) $0 < A_{12} < 0.16$ erg/cm², $|k| = 18 \mu\text{m}^{-1}$; circles indicate the frequency difference obtained with the asymptotic expression $\frac{2\gamma}{\pi} \frac{D}{M_1 t_{\text{FM}_1} + M_2 t_{\text{FM}_2}} k$.

mode increases and the one associated to the exchange mode $f_2(-k) - f_2(k)$ decreases. For a very high value of the exchange coupling $A_{12} = 10$ erg/cm², the highest frequency f_2 is out of the BLS experimental range while the lowest frequency f_1 is still observable and the frequency difference $f_1(-k) - f_1(k)$ coincides with $\delta f_{\text{mean}} = \frac{2\gamma}{\pi} \frac{D}{t_{\text{FM}_1} M_1 + t_{\text{FM}_2} M_2} k$. This suggests that for a vanishing spacer, the bilayer FM₂/FM₁ behaves like one layer with a thickness $t_{\text{FM}_1} + t_{\text{FM}_2}$ and a magnetization $\frac{t_{\text{FM}_1} M_1 + t_{\text{FM}_2} M_2}{t_{\text{FM}_1} + t_{\text{FM}_2}}$. Finally the iDMI effect should be easy to quantify for a FM₂/FM₁/HM stack like in the case of FM/HM bilayer.

F. (NM/FM)₄/HM

In order to illustrate the shift of frequency induced by iDMI in a repetition of nonmagnetic (NM)/ferromagnetic (FM) bilayers with the bottom FM layer in contact with the heavy metal (HM), calculations were made for four (NM/FM) bilayers where the thickness of one FM film was identical and fixed to $t_{\text{FM}} = 2$ nm, and separated by 0.2-nm-thick NM spacers. The calculated dispersion laws of the four modes resulting from the coupling are displayed in Fig. 8. They were obtained with the following parameters: $H = 1000$ Oe, $M = 1000$ emu/cc, $A = 10^{-6}$ erg/cm, $D = 0$ or 10^{-7} erg/cm, and $\frac{\gamma}{2\pi} = 3$ GHz/kOe, $K = K_{s,\text{up}} = K_{s,\text{low}} = 0$, $A_{12} = 0.02$ erg/cm². The order of magnitude of the shift of frequency due to iDMI is about $(\gamma/\pi)[D/(4tM)]k$. Nevertheless this estimation is largely disturbed by the coupling of the dipolar

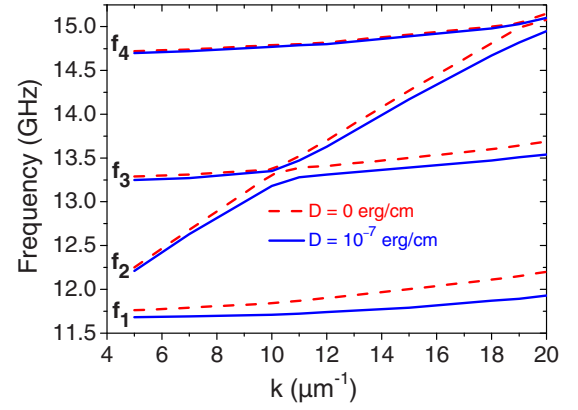


FIG. 8. Dispersion laws for four identical coupled magnetic films on a layer inducing iDMI. The coupling results in four modes represented for $D = 0$ (dashed lines) and $D = 10^{-7}$ erg/cm (plain lines).

mode, which is the most wave-number dependent one, with the three other modes representing the exchange modes. In the case of a multilayer, the iDMI shift of the frequency is not proportional to the wave number and depends on the mode. Its evaluation requires a complete calculation of the frequency. The frequency shift due to iDMI is presented in Table I. The frequencies are labeled as an increasing series $f_1 < f_2 < f_3 < f_4$.

IV. APPROXIMATE EXPLICIT EXPRESSIONS FOR THE FREQUENCIES OF EIGENMODES IN MULTILAYERS MADE OF FERROMAGNETS, NORMAL METAL, AND HEAVY METAL

The purpose of this section is to derive formulas for eigenfrequencies with a method similar to that used to obtain the usual expression in the case of one layer. Such an expression can be derived only for stacks made of identical magnetic layers. In this case, these explicit expressions are in agreement with numerical results. The frequencies are derived by averaging the motion equation (like in Ref. [40]). In the case of a single layer the averaged equation of motion reads

$$\begin{aligned} & i \left(\frac{\omega}{\gamma} + k \frac{2D_{\text{eff}}}{M} \right) \vec{m} \\ &= \vec{M} \times \left[-\frac{2A}{M^2} k^2 \vec{m} - 4\pi(1-G)m_x \vec{u}_x - 4\pi G m_y \vec{u}_y \right. \\ & \quad \left. + \frac{2K_{\text{eff}}}{M^2} m_y \vec{u}_y \right] + \vec{m} \times \vec{H} \end{aligned} \quad (22)$$

with $G = \frac{1 - \exp(-|k|t)}{|k|t}$, $D_{\text{eff}} = \frac{D_s}{t}$, $K_{\text{eff}} = K + \frac{k_s}{t}$, where D_s and k_s are associated to both upper and lower interfaces. $k_s =$

TABLE I. Frequency shift for $k_0 = 5 \mu\text{m}^{-1}$ and $3k_0 = 15 \mu\text{m}^{-1}$.

n	1	2	3	4
$f_n(k_0, 0) - f_n(k_0, D)$ (GHz)	0.08	0.04	0.04	0.02
$f_n(3k_0, 0) - f_n(3k_0, D)$ (GHz)	0.21	0.11	0.10	0.02

$K_{s,\text{low}} + K_{s,\text{up}}$ is simply the sum of lower and upper surface anisotropies. Because of the averaging of LL equation, the surface anisotropy contribution k_s/t and the bulk contribution K cannot be separated and yield an effective bulk contribution K_{eff} . In Sec. II, iDMI was localized only at the lower interface and the corresponding constant was D . In this case $D_s = D$. Nonetheless, if both upper and lower interfaces are involved in iDMI then $D_s = D_{\text{up}} + D_{\text{low}}$ is the algebraic sum of both contributions. It should be noticed that if the same heavy metal is present at both interfaces then $D_{\text{up}} = -D_{\text{low}}$ thus $D_s = 0$ [26]. At variance, if the same metal is present at both interfaces $K_{s,\text{low}} = K_{s,\text{up}}$ and $k_s = 2K_{s,\text{low}}$.

From Eq. (22), one obtains

$$\left(\frac{\omega}{\gamma} + \frac{2D_{\text{eff}}}{M}k\right)^2 = H_x H_y \quad (23)$$

with $H_x = H + \frac{2A}{M}k^2 + 4\pi(1-G)M$ and $H_y = H + \frac{2A}{M}k^2 + 4\pi GM - \frac{2K_{\text{eff}}}{M}$. Consequently the frequency difference reads $\frac{1}{2\pi}[\omega(k) - \omega(-k)] = -\frac{2\gamma D_{\text{eff}}k}{\pi M}$.

A. Calculation of the dipolar coupling

In the case of two coupled layers, the stray field engendered by each layer is to be estimated. This calculation will be performed using the same method as that providing the demagnetizing factor G . The first step consists in deriving the perpendicular component of the field generated by an oscillatory magnetization uniform across the thickness,

$$h_y(x, y) = \int \int m_y \exp(ikx') \times \left(\frac{y-t/2}{[(x-x')^2 + (y-t/2)^2 + (z')^2]^{3/2}} - \frac{y+t/2}{[(x-x')^2 + (y+t/2)^2 + (z')^2]^{3/2}} \right) dx' dz'. \quad (24)$$

Using the property $\frac{d}{du} \left(\frac{u}{\sqrt{u^2+c^2}} \right) = \frac{c^2}{(u^2+c^2)^{3/2}}$, one obtains

$$h_y(x, y) = \int 2m_y \exp(ikx') \left(\frac{y-t/2}{(x-x')^2 + (y-t/2)^2} - \frac{y+t/2}{(x-x')^2 + (y+t/2)^2} \right) dx'. \quad (25)$$

Using the relation $\int \frac{\exp(iku)}{u^2+c^2} du = \pi \exp(-|kc|)/|c|$, one deduces

$$h_y(x, y) = 2\pi m_y \left\{ \exp[ikx - |k(y-t/2)|] \frac{y-t/2}{|y-t/2|} - \exp[ikx - |k(y+t/2)|] \frac{y+t/2}{|y+t/2|} \right\}. \quad (26)$$

The second step consists in averaging $h_y(x, y)$ over the appropriate y range. For $y > t/2$,

$$h_y(x, y) = 2\pi m_y \{ \exp[ikx - |k|(y-t/2)] - \exp[ikx - |k|(y+t/2)] \} \quad (27)$$

thus the average value over the range $t/2 + s < y < 3t/2 + s$ corresponding to a s distant overlayer reads

$$h_y(x) = 2\pi m_y \exp(ikx) \exp(-|k|s) \frac{[1 - \exp(-|k|t)]^2}{|k|t}. \quad (28)$$

We set $F = \frac{1}{2} \exp(-|k|s) \frac{[1 - \exp(-|k|t)]^2}{kt}$, thus $h_y(x) = 4\pi F m_y \exp(ikx)$.

Inside the layer where the magnetization lies, $-t/2 < y < t/2$ and

$$h_y(x, y) = 2\pi m_y \{ -\exp[ikx - |k|(t/2 - y)] - \exp[ikx - |k|(y + t/2)] \} \quad (29)$$

thus the average value reads $-4\pi m_y \exp(ikx) \frac{1 - \exp(-|k|t)}{|k|t}$. We set $G = \frac{1 - \exp(-|k|t)}{|k|t}$, thus $h_y(x) = -4\pi G m_y \exp(ikx)$.

The final step consists in using the relation between demagnetizing factors: inside the layer where lies the magnetization $h_x = -4\pi(1-G)m_x$ while inside the overlayer $h_x = -4\pi F m_x$.

B. (FM/NM/FM/HM) stack

The dipolar field is supposed to be the only source of coupling between FM layers. In this case, the coupled equations of motion read, in the film in contact with the heavy metal,

$$i \left(\frac{\omega}{\gamma} + \frac{2D_{\text{eff}}}{M}k \right) \vec{m}_1 = \vec{M} \times \left[-\frac{2A}{M^2}k^2 \vec{m}_1 - 4\pi(1-G)m_{x,1} \vec{u}_x - 4\pi G m_{y,1} \vec{u}_y + \frac{2K_{\text{eff}}}{M^2} m_{1,y} \vec{u}_y \right] + \vec{m}_1 \times \vec{H} + \vec{M} \times (-4\pi F m_{2,x} \vec{u}_x + 4\pi F m_{2,y} \vec{u}_y), \quad (30)$$

and in the upper ferromagnetic layer,

$$i \frac{\omega}{\gamma} \vec{m}_2 = \vec{M} \times \left[-\frac{2A}{M^2}k^2 \vec{m}_2 - 4\pi(1-G)m_{x,2} \vec{u}_x - 4\pi G m_{y,2} \vec{u}_y + \frac{2K_{\text{eff}}}{M^2} m_{2,y} \vec{u}_y \right] + \vec{m}_2 \times \vec{H} + \vec{M} \times (-4\pi F m_{1,x} \vec{u}_x + 4\pi F m_{1,y} \vec{u}_y). \quad (31)$$

One can rewrite these relations in the following way:

$$\begin{pmatrix} i(H_\omega + H_{DMI}) & -H_y \\ H_x & i(H_\omega + H_{DMI}) \end{pmatrix} \begin{pmatrix} m_{x,1} \\ m_{y,1} \end{pmatrix} = \begin{pmatrix} 0 & -H_c \\ -H_c & 0 \end{pmatrix} \begin{pmatrix} m_{x,2} \\ m_{y,2} \end{pmatrix} \quad (32)$$

and

$$\begin{pmatrix} i(H_\omega) & -H_y \\ H_x & i(H_\omega) \end{pmatrix} \begin{pmatrix} m_{x,2} \\ m_{y,2} \end{pmatrix} = \begin{pmatrix} 0 & -H_c \\ -H_c & 0 \end{pmatrix} \begin{pmatrix} m_{x,1} \\ m_{y,1} \end{pmatrix}, \quad (33)$$

where $H_\omega = \frac{\omega}{\gamma}$, $H_{DMI} = \frac{2D_{\text{eff}}}{M}k$, $H_c = 4\pi FM$.

As

$$\begin{pmatrix} 0 & -H_c \\ -H_c & 0 \end{pmatrix} \begin{pmatrix} 0 & -H_c \\ -H_c & 0 \end{pmatrix} = (H_c)^2 \begin{pmatrix} 1 & 0 \\ 0 & 1 \end{pmatrix} \quad (34)$$

one deduces

$$\begin{pmatrix} -H_c H_x & -i H_c (H_\omega + H_{DMI}) \\ -i H_c (H_\omega + H_{DMI}) & H_c H_y \end{pmatrix} \begin{pmatrix} -H_c H_x & -i H_c H_\omega \\ -i H_c H_\omega & H_c H_y \end{pmatrix} \begin{pmatrix} m_{x,2} \\ m_{y,2} \end{pmatrix} = (H_c)^4 \begin{pmatrix} m_{x,2} \\ m_{y,2} \end{pmatrix}. \quad (35)$$

Consequently the eigenfrequencies are associated to the condition

$$\begin{vmatrix} H_c^2 H_x^2 - H_c^2 H_\omega (H_\omega + H_{DMI}) - H_c^4 & i H_c^2 H_x H_\omega - i H_c^2 H_y (H_\omega + H_{DMI}) \\ i H_c^2 H_x (H_\omega + H_{DMI}) - i H_c^2 H_y H_\omega & H_c^2 H_y^2 - H_c^2 H_\omega (H_\omega + H_{DMI}) - H_c^4 \end{vmatrix} = 0. \quad (36)$$

Finally

$$(H_\omega + \frac{1}{2} H_{DMI})^2 = H_x H_y + \frac{1}{4} H_{DMI}^2 - H_c^2 \pm \sqrt{H_x H_y H_{DMI}^2 + H_c^2 (H_x - H_y)^2}. \quad (37)$$

This expression implies that $(H_\omega + \frac{1}{2} H_{DMI})(-k) = (H_\omega + \frac{1}{2} H_{DMI})(k)$. Consequently the frequency difference $\frac{1}{2\pi} [\omega(k) - \omega(-k)] = -\frac{\gamma D_{\text{eff}} k}{\pi M}$ is the half difference for one ferromagnetic layer on a heavy metal.

C. Multiple (HM₁/FM/HM₂) stack

In this section, we consider a stack of identical ferromagnetic layers where each layer is sandwiched between two different heavy metal layers, $n \times (\text{HM}_1/\text{FM}/\text{HM}_2)$. In this case one obtains the same frequency difference for any value of n .

1. Two coupled identical layers

The coupled equations of motion read as follows: in the film labeled by 1, $i(\frac{\omega}{\gamma} + k \frac{2D_{\text{eff}}}{M}) \vec{m}_1 = \vec{M} \times [-\frac{2A}{M^2} k^2 \vec{m}_1 - 4\pi(1-G)m_{x,1} \vec{u}_x - 4\pi G m_{y,1} \vec{u}_y + \frac{2K_{\text{eff}}}{M^2} m_{1,y} \vec{u}_y] + \vec{m}_1 \times \vec{H} + \vec{M} \times (-4\pi F m_{2,x} \vec{u}_x + 4\pi F m_{2,y} \vec{u}_y)$ and in the film labeled by 2, $i(\frac{\omega}{\gamma} + k \frac{2D_{\text{eff}}}{M}) \vec{m}_2 = \vec{M} \times [-\frac{2A}{M^2} k^2 \vec{m}_2 - 4\pi(1-G)m_{x,2} \vec{u}_x - 4\pi G m_{y,2} \vec{u}_y + \frac{2K_{\text{eff}}}{M^2} m_{2,y} \vec{u}_y] + \vec{m}_2 \times \vec{H} + \vec{M} \times (-4\pi F m_{1,x} \vec{u}_x + 4\pi F m_{1,y} \vec{u}_y)$. From these relations, one obtains $(\frac{\omega}{\gamma} + k \frac{2D_{\text{eff}}}{M})^2 = H_x H_y - (4\pi F M)^2 \pm 4\pi M F (H_x - H_y)$. This relation is similar to that obtained for one layer. The frequency difference $\frac{\omega(k) - \omega(-k)}{2\pi}$ has exactly the same expression in both cases: it reads $-\frac{\gamma}{\pi} \frac{2D_{\text{eff}}}{M} k$ where D_{eff} is the surface DMI constant for one layer.

2. Several coupled identical layers

In the case of several coupled layers, a similar calculation yields the same conclusion for the frequency difference: if the stack is made of identical layers with identical environment, then the frequency difference is that of one single layer. The coupled equations can be written $i(H_\omega + H_{DMI})m_{p,x} = H_y m_{p,y} - \sum_q 4\pi F_q m_{q,y}$, $i(H_\omega + H_{DMI})m_{p,y} = -H_x m_{p,x} - \sum_q 4\pi F_q m_{q,x}$, where $H_{DMI} = \frac{2D_{\text{eff}}}{M} k$ and $H_\omega = \frac{\omega}{\gamma}$.

Consequently $i(H_\omega + H_{DMI})$ is an eigenvalue of a matrix independent on the k sign.

Consequently $(H_\omega + H_{DMI})(-k) = (H_\omega + H_{DMI})(k)$ and the frequency difference $\frac{1}{2\pi} [\omega(k) - \omega(-k)]$ is equal to $-\frac{\gamma}{\pi} \frac{2D_{\text{eff}}}{M} k$ like in one single layer.

V. ANALYSIS OF EXPERIMENTAL DATA

We present in this section some experimental results obtained by using the Brillouin light scattering (BLS) technique and analyzed by means of the above model.

A. Thin ferromagnetic (FM)/heavy metal (HM)

We have investigated the spin-wave nonreciprocity in a Pt/CoFeB bilayer deposited by sputtering technique on thermally oxidized silicon substrate within a stack of the following composition: Si/SiO₂/Pt(2 nm)/CoFeB(0.8 nm)/MgO(2 nm)/SiO₂(3 nm). The Stokes $f(-k)$ and anti-Stokes $f(k)$ frequencies have been measured in the Damon-Eshbach configuration, for a wave number $|k|$ varying from 4 to 20 μm^{-1} . A frequency difference was observed between the Stokes and anti-Stokes lines, as presented in Fig. 9, and was found to increase linearly with k (see inset). This behavior is of course ascribed to the iDMI generated at the Pt/CoFeB interface. Indeed, for such low thickness, the surface anisotropy contribution to the spin waves nonreciprocity is negligible in comparison with the one generated by the iDMI [43,48]. From the derived expression of the frequency difference $f(-k) - f(k) = \frac{2\gamma}{\pi M} \frac{D}{t_{\text{FM}}} k$ [see Refs. [34,35,49,50] and Eq. (22)], and using the following parameters: $M = 1600$ emu/cc obtained from VSM

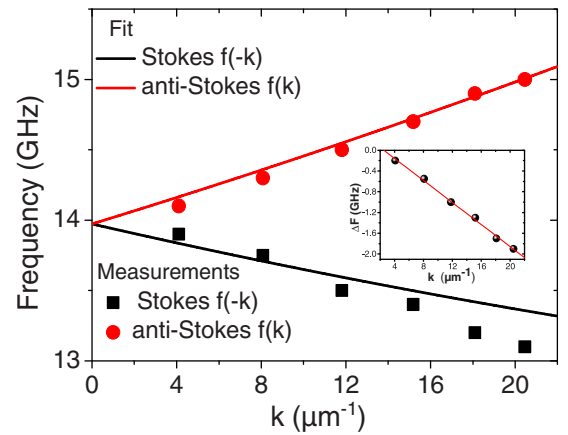


FIG. 9. Variation of the experimental Stokes $f(-k)$ and anti-Stokes $f(k)$ frequencies of Pt/CoFeB(0.8 nm) vs the in-plane wave number k , obtained for a 7-kOe in-plane magnetic field. Solid lines refer to fits using the model described in the paper. Inset shows the frequency difference $f(k) - f(-k)$ as function of k .

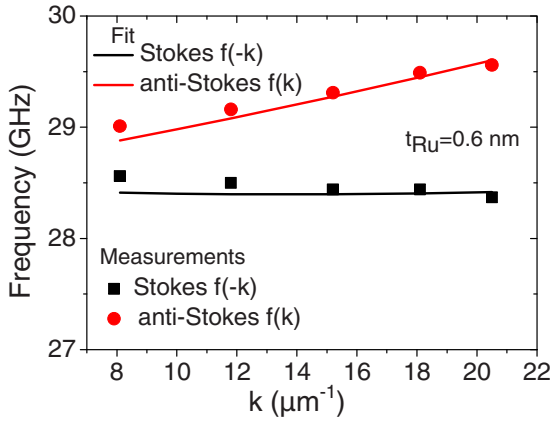


FIG. 10. Variation of the experimental Stokes $f(-k)$ and anti-Stokes $f(k)$ frequencies of the dipolar mode of CoFeB(1.12 nm)/Ru(0.6 nm)/CoFeB(1.12 nm)/Pt vs the in-plane wave number k , obtained for 5-kOe in-plane magnetic field. Solid lines refer to fits using the model described in the text.

measurements [48], $\frac{\gamma}{2\pi} = 3.01 \times 10^{-3}$ GHz/Oe, we obtain an interfacial DMI constant $D = -0.8 \times 10^{-7}$ erg/cm ($= -0.8$ pJ/m), in line with the value previously reported [48].

B. Heavy metal (HM)/ferromagnetic (FM)/normal metal (NM)/ferromagnetic (FM)

Two samples are considered: Pt/CoFeB/Ru/CoFeB, where the interlayer exchange coupling is negative (antiferromagnetic coupling), $A_{12} < 0$, and Co/Cu/Co/Pt where it is positive, $A_{12} > 0$. In both cases, the coupled ferromagnetic layers have different anisotropies because of different neighboring layers. Our numerical calculations show that in such structures the spin-wave nonreciprocity $f(-k) - f(k)$ is also influenced by the anisotropy difference and by the interlayer exchange coupling.

1. Pt/CoFeB/Ru/CoFeB/MgO

The studied sample is made of two CoFeB 1.12-nm-thick layers coupled through a Ru 0.6-nm-thick layer. The magnetization at saturation $M = 1200$ emu/cc was measured by magnetometry. The negative exchange coupling $A_{12} = -0.1$ erg/cm² (antiferromagnetic coupling) was experimentally evidenced on hysteresis loops obtained with an in-plane applied field [51]. The gyromagnetic factor $\frac{\gamma}{2\pi} = 3.01 \times 10^{-3}$ GHz/Oe was deduced from FMR experiments [51]. BLS has been used to measure their dispersion relation for an in-plane applied magnetic field largely enough to saturate the magnetization in the film plane. Only the dipolar mode has been observed due to the weak intensity of the optic mode resulting from the similarly coupled ferromagnetic CoFeB films. As shown in Ref. [51], the frequency difference of such systems depends on the Ru thickness (coupling), suggesting that the two CoFeB layers are not similar despite their similar thicknesses. Indeed, different cap and/or buffer layers are used for the two CoFeB implying a different interface anisotropy in the CoFeB films. Therefore, the iDMI constant $D = -0.93 \times 10^{-7}$ erg/cm was determined from the BLS measurement of Pt/CoFeB/Ru structure [51]. Finally, using the

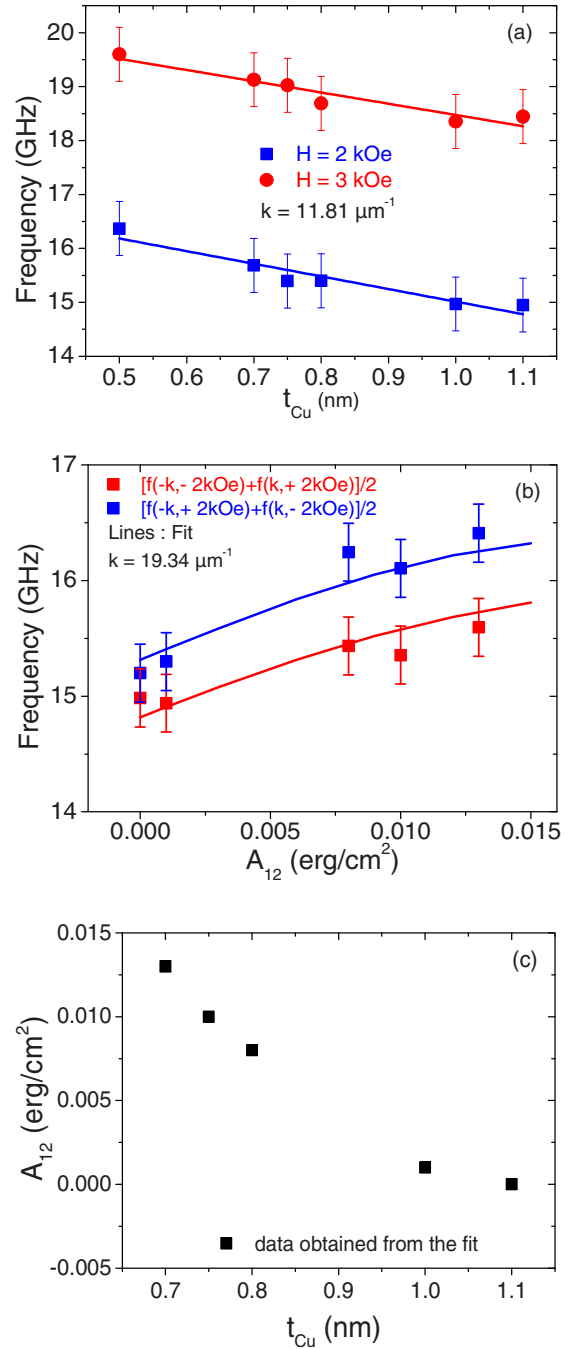


FIG. 11. (a) Measured frequencies at 2 and 3 kOe with a wave number $k = 11.81 \mu\text{m}^{-1}$ vs the Cu thickness; (b) theoretical variations of the Stokes and anti-Stokes frequencies vs A_{12} ($H = \pm 2$ kOe, $k = 19.34 \mu\text{m}^{-1}$) and experimental data (average frequencies obtained for ± 2 kOe), $[f(-k, -2 \text{ kOe}) + f(k, +2 \text{ kOe})]/2$ and $[f(-k, +2 \text{ kOe}) + f(k, -2 \text{ kOe})]/2$; (c) A_{12} vs t_{Cu} .

above-mentioned value of the iDMI constant, the anisotropies in the two FM layers $H_{a,FM2} = 10900$ Oe, $H_{a,FM1} = 8900$ Oe were evaluated by fitting the frequency variations with respect to the wave vector for the dipolar mode line. The experimental data and the fitting curves are displayed in Fig. 10. This example shows that the frequency difference $f(-k) - f(k)$ for coupled FM layers does not allow for directly evaluating

the iDMI constant. Indeed, due to the ultrathin films needed for inducing iDMI, the interface anisotropy could be significant, therefore, the degeneracy of the two FM layers is lifted leading to an additional fit parameter (interface anisotropy). As a matter of fact, the different surface anisotropies yield different effective anisotropies in the two FM layers. As discussed in Sec. III E, for two different FM layers, the frequency difference depends on A_{12} .

2. MgO/Co/Cu/Co/Pt

The studied samples correspond to the following stacks: substrate/MgO(2)/Co(1.2)/Cu(t_{Cu})/Co(1.2)/Pt(4) (thicknesses in nanometers), with Cu thickness t_{Cu} varying between 0.7 and 1.1 nm, in order to point out the influence of the magnetic exchange coupling. The magnetization, measured by magnetometry, was found to slightly vary around $M_s = 1200$ emu/cc with t_{Cu} . This apparent saturation magnetization is lower than that of bulk Co (=1400 emu/cc). We assumed that a dead layer exists at the interface with MgO as previously reported for other systems [26]. Consequently, the real thickness of the buried Co layer was taken equal to 0.85 nm. Hysteresis loops in the in-plane magnetic field configuration evidenced a positive exchange coupling A_{12} (ferromagnetic coupling). BLS experiments were performed with wave number $k = 20.45 \mu\text{m}^{-1}$ using a saturating positive and negative applied magnetic field of ± 3 kOe in order to evaluate the iDMI constant from Stokes and anti-Stokes frequency difference of the sole observable dipolar line. The gyromagnetic factor $\gamma/2\pi = 2.9 \times 10^{-3}$ GHz/Oe was deduced from FMR measurements. The iDMI constant was estimated to be $D = 10^{-7}$ erg/cm for all the samples, assuming that it mainly originates from the Co/Pt interface. This value is slightly inferior to that obtained when Pt is buried. Such behavior is conformal to previously reported results [38,52]. Moreover, BLS measurements at lower wave number $k = 11.81 \mu\text{m}^{-1}$, using applied magnetic fields varying from 2 to 4 kOe, were performed in order to evaluate the effective magnetization. The frequency measurements could be interpreted assuming that the capping and buffer layers present two different anisotropies: ($H_{a,FM1}$) for Co layer in contact with Pt and ($H_{a,FM2}$) for the one in contact with MgO. Due to the fact that the interface Cu/Co or Co/Cu induces a weak surface anisotropy [53], it is fair to assume that the interface anisotropy is mainly due to the MgO/Co and Co/Pt interfaces.

Therefore we could assume that ($H_{a,FM1}$) and ($H_{a,FM2}$) are constant for all the samples: $H_{a,FM1} = 6800$ Oe, $H_{a,FM2} = 6500$ Oe. Moreover, the frequency difference can be fitted only considering $H_{a,FM1} > H_{a,FM2}$ [53,54], otherwise the frequency difference would be too low. Figure 11(a) presents the measured frequencies at 2 and 3 kOe with a wave number $k = 11.81 \mu\text{m}^{-1}$ versus the Cu thickness. The frequencies slightly decrease when t_{Cu} increases. This behavior was related to the A_{12} dependence with respect to t_{Cu} . Consequently we present in Fig. 11(b), the theoretical variations of the Stokes and anti-Stokes frequencies versus A_{12} and plot for $k = 19.34 \mu\text{m}^{-1}$ the experimental data (average frequencies obtained for ± 2 kOe), $[f(-k, -2k\text{Oe}) + f(k, +2k\text{Oe})]/2$ and $[f(-k, +2k\text{Oe}) + f(k, -2k\text{Oe})]/2$ in order to determine A_{12} for each sample. Finally we plot A_{12} versus t_{Cu} in Fig. 11(c). The observed variation of A_{12} vs t_{Cu} is in line with results reported in Ref. [45].

VI. CONCLUSION

This paper presents a full calculation of spin-wave frequency in multilayers where one magnetic layer experiences an interfacial Dzyaloshinskii-Moriya interaction. Such a complete calculation is necessary in complex structures to accurately estimate the magnitude of this interaction. The usual simple formula relating this magnitude to the slope of the spin-wave nonreciprocity versus the wave number is not valid in many real structures. In the case of stacks made of identical magnetic layers, we checked thanks to an analytical calculation that the effect of iDMI on the entire structure is captured by including the total thickness of the ferromagnetic layers. These expressions are useful to discuss numerical results. Some experimental data obtained for various systems by means of Brillouin light scattering are analyzed through the presented models.

ACKNOWLEDGMENTS

This work has been supported by the Conseil régional d'Île-de-France through the DIM Nano-K (Bidul project, convention n° 1763, 2016 NANO-K DIM programme), by the National Research Foundation (NRF) Singapore under its Competitive Research Programme (NRF-CRP12-2013-01), and by the USPC-NUS alliance (Imansa project, 2016-01-R/USPC-NUS).

-
- [1] E. Dzyaloshinskii, *J. Phys. Chem. Solids* **4**, 241 (1958).
 [2] T. Moriya, *Phys. Rev.* **120**, 91 (1960).
 [3] A. Fert and P.-M. Levy, *Phys. Rev. Lett.* **44**, 1538 (1980).
 [4] A. Fert, *Mater. Sci. Forum* **439**, 59 (1990).
 [5] S. S. P. Parkin, M. Hayasi, and L. Thomas, *Science* **320**, 190 (2008).
 [6] A. Fert, V. Cros, and J. Sampaio, *Nat. Nanotechnol.* **8**, 152 (2013).
 [7] N. Nagaosa and Y. Tokura, *Nat. Nanotechnol.* **8**, 899 (2013).
 [8] R. Wiesendanger, *Nat. Rev. Mater.* **1**, 16044 (2016).
 [9] F. Hellman, A. Hoffman, Y. Tserkovnyak, G. Beach, E. Fullerton, C. Leighton, A. MacDonald, D. Ralph, D. Arena, H. Dürr, P. Fisher, J. Grolier, P. Heremans, T. Jungwirth, A. Kimel, B. Koopmans, I. Krivorotov, S. May, A. Petford-Long, J. Rondinelli *et al.*, *Rev. Mod. Phys.* **89**, 025006 (2017).
 [10] G. Chen, A. Mascaraque, A. N'Diaye, and A. Schmid, *Appl. Phys. Lett.* **106**, 242404 (2015).
 [11] C. Moreau-Lucaire, C. Moutafis, N. Reyren, J. Sampaio, C. Vaz, N. V. Hone, K. Bouzehouane, K. Garcia, C. Deranlot, P. Warnicke, P. Wohlhueter, J.-M. George, M. Weigand, J. Raabe, V. Cros, and A. Fert, *Nat. Nanotechnol.* **11**, 444 (2016).
 [12] O. Boule, J. Vogel, H. Yang, S. Pizzini, D. de Souza Chaves, A. Locatelli, T. Mentès, A. Sala, L. Buda-Prejbeanu, O. Klein, M. Belmeguenai, Y. Roussigné, A. Stashkevich, S. M. Chérif,

- L. Aballe, M. Foerster, M. Chshiev, S. Auffret, I. Miron, and G. Gaudin, *Nat. Nanotechnol.* **11**, 898 (2016).
- [13] A. Soumyanarayanan, M. Raju, A. L. Gonzalez Oyarce, A. Tan, M. Im, A. Petrovic, P. Ho, K. Khoo, M. Tran, C. Gan, F. Ernult, and C. Panagopoulos, *Nat. Mater.* **16**, 898 (2017).
- [14] S. D. Pollard, J. A. Garlow, J. Yu, Z. Wang, Y. Zhu, and H. Yang, *Nat. Commun.* **8**, 14761 (2017).
- [15] A. Hrabec, J. Sampaio, M. Belmeguenai, I. Gross, R. Weil, S. M. Chérif, A. Stashkevich, V. Jacques, A. Thiaville, and S. Rohart, *Nat. Commun.* **8**, 15765 (2017).
- [16] W. Legrand, D. Maccariello, N. Reyren, K. Garcia, C. Moutafis, C. Moreau-Luchaire, S. Collin, K. Bouzehouane, V. Cros, and A. Fert, *Nano Lett.* **17**, 2703 (2017).
- [17] S. Emori, U. Bauer, S. Ahn, E. Martinez, and G. Beach, *Nat. Mater.* **12**, 611 (2013).
- [18] E. Jué, A. Thiaville, S. Pizzini, J. Miltat, J. Sampaio, L. D. Buda-Prejbeanu, S. Rohart, J. Vogel, M. Bonfim, O. Boulle, S. Auffret, I. M. Miron, and G. Gaudin, *Phys. Rev. B* **93**, 014403 (2016).
- [19] K.-J. Kim, Y. Yoshimura, T. Okuno, T. Moriyama, S.-W. Lee, K.-J. Lee, Y. Nakatani, and T. Ono, *APL Mater.* **4**, 032504 (2016).
- [20] R. Soucaille, M. Belmeguenai, J. Torrejon, J.-V. Kim, T. Devolder, Y. Roussigné, S.-M. Chérif, A. A. Stashkevich, M. Hayashi, and J.-P. Adam, *Phys. Rev. B* **94**, 104431 (2016).
- [21] P. Sethi, S. Krishnia, W. L. Gan, F. N. Kholid, F. N. Tan, R. Maddu, and W. S. Lew, *Sci. Rep.* **7**, 4964 (2017).
- [22] J. Iwasaki, M. Mochizuki, and N. Nagaosa, *Nat. Nanotechnol.* **8**, 742 (2013).
- [23] S. Woo, K. Litzius, B. Krüger, M.-Y. Im, L. Caretta, K. Richter, M. Mann, A. Krone, R. M. Reeve, M. Weigand, P. Agrawal, I. Lemesch, M.-A. Mawass, P. Fischer, M. Kläui, and G. Beach, *Nat. Mater.* **15**, 501 (2016).
- [24] G. Chen, T. Ma, A. N'Diaye, H. Kwon, C. Won, Y. Wu, and A. K. Schmid, *Nat. Commun.* **4**, 2671 (2013).
- [25] X. Ma, G. Yu, X. Li, T. Wang, D. Wu, K. S. Olsson, Z. Chu, K. An, J. Q. Xiao, K. L. Wang, and X. Li, *Phys. Rev. B* **94**, 180408(R) (2016).
- [26] M. Belmeguenai, M. S. Gabor, Y. Roussigné, A. Stashkevich, S. M. Chérif, F. Zighem, and C. Tiusan, *Phys. Rev. B* **93**, 174407 (2016).
- [27] M. Quinsat, Y. Ootera, T. Shimada, M. Kado, S. Hashimoto, H. Morise, S. Nakamura, and T. Kondo, *AIP Adv.* **7**, 056318 (2017).
- [28] A. W. J. Wells, P. M. Shepley, C. H. Marrows, and T. A. Moore, *Phys. Rev. B* **95**, 054428 (2017).
- [29] H. Yang, A. Thiaville, S. Rohart, A. Fert, and M. Chshiev, *Phys. Rev. Lett.* **115**, 267210 (2015).
- [30] P. Grünberg, R. Schreiber, Y. Pang, M. B. Brodsky, and H. Sowers, *Phys. Rev. Lett.* **57**, 2442 (1986).
- [31] M. Vohl, J. Barnaś, and P. Grünberg, *Phys. Rev. B* **39**, 12003 (1989).
- [32] S. Demokritov, J. A. Wolf, and P. Grünberg, *Europhys. Lett.* **15**, 881 (1991).
- [33] M. Buchmeier, B. K. Kuanr, R. R. Gareev, D. E. Bürgler, and P. Grünberg, *Phys. Rev. B* **67**, 184404 (2003).
- [34] M. Belmeguenai, J.-P. Adam, Y. Roussigné, S. Eimer, T. Devolder, J.-V. Kim, S. M. Chérif, A. Stashkevich, and A. Thiaville, *Phys. Rev. B* **91**, 180405(R) (2015).
- [35] K. Di, V. L. Zhang, H. S. Lim, S. C. Ng, M. H. Kuok, J. Yu, J. Yoon, X. Qiu, and H. Yang, *Phys. Rev. Lett.* **114**, 047201 (2015).
- [36] J. Cho, N.-H. Kim, S. Lee, J.-S. Kim, R. Lavrijsen, A. Solignac, Y. Yin, D.-S. Han, N. van Hoof, H. Swagten, B. Koopmans, and C.-Y. You, *Nat. Commun.* **6**, 7635 (2015).
- [37] H. T. Nembach, J. Shaw, M. Weiler, E. Jué, and T. J. Silva, *Nat. Phys.* **11**, 825 (2015).
- [38] N.-H. Kim, J. Jung, J. Cho, D.-S. Han, Y. Yin, J.-S. Kim, H. Swagten, and C.-Y. You, *Appl. Phys. Lett.* **108**, 142406 (2016).
- [39] B. Hillebrands, *Phys. Rev. B* **41**, 530 (1990).
- [40] M. Kostylev, *J. Appl. Phys.* **115**, 233902 (2014).
- [41] R. Arias and D. L. Mills, *Phys. Rev. B* **60**, 7395 (1999).
- [42] R. E. Camley and D. L. Mills, *Phys. Rev. B* **18**, 4821 (1978).
- [43] A. A. Stashkevich, M. Belmeguenai, Y. Roussigné, S. M. Chérif, M. Kostylev, M. Gabor, D. Lacour, C. Tiusan, and M. Hehn, *Phys. Rev. B* **91**, 214409 (2015).
- [44] F. Hoffmann, *Phys. Status Solidi* **41**, 807 (1970).
- [45] S. S. P. Parkin, *Phys. Rev. Lett.* **67**, 3598 (1991).
- [46] S. S. P. Parkin and D. Mauri, *Phys. Rev. B* **44**, 7131 (1991).
- [47] P. Bruno and C. Chappert, *Phys. Rev. B* **46**, 261 (1992).
- [48] K. Di, V. L. Zhang, H. S. Lim, S. C. Ng, M. H. Kuok, X. Qiu, and H. Yang, *Appl. Phys. Lett.* **106**, 052403 (2015).
- [49] J.-H. Moon, S.-M. Seo, K.-J. Lee, K.-W. Kim, J. Ryu, H.-W. Lee, R. D. McMichael, and M. D. Stiles, *Phys. Rev. B* **88**, 184404 (2013).
- [50] D. Cortés-Ortuño and P. Landeros, *J. Phys.: Condens. Matter* **25**, 156001 (2013).
- [51] M. Belmeguenai, H. Bouloussa, Y. Roussigné, M. S. Gabor, T. Petrisor, Jr., C. Tiusan, H. Yang, A. Stashkevich, and S. M. Chérif, *Phys. Rev. B* **96**, 144402 (2017).
- [52] R. Rowan-Robinson, A. Stashkevich, Y. Roussigné, M. Belmeguenai, S. M. Chérif, A. Thiaville, T. Hase, A. Hindmarch, and D. Atkinson, *Sci. Rep.* **7**, 16835 (2017).
- [53] M. Johnson, P. Bloeman, F. den Broeder, and J. de Vries, *Rep. Prog. Phys.* **59**, 1409 (1996).
- [54] J.-W. Cai, S. Okamoto, O. Kitakami, and Y. Shimada, *Phys. Rev. B* **63**, 104418 (2001).